Formation and evolution of small B clusters in Si: Ion channeling study

Lucia Romano,[1,2] Alberto Maria Piro,[1,2] Salvatore Mirabella,[1] and Maria Grazia Grimaldi[1,2]
[1]*MATIS CNR-INFM, Via S. Sofia 64, I-95123 Catania, Italy*
[2]*Dipartimento di Fisica e Astronomia, Università di Catania, Via S. Sofia 64, I-95123 Catania, Italy*
(Received 5 December 2008; revised manuscript received 23 April 2009; published 17 February 2010)

B off-lattice displacement in B-doped Si was observed under Si self-interstitials (*Is*) supersaturation induced by ion irradiation at room temperature. B lattice location has a characteristic channeling mark and was studied by nuclear reaction analyses and ion channeling technique, through the comparison of the performed angular scans along the ⟨100⟩ and ⟨110⟩ crystal axes and the simulated scans by FLUX code. Solid and liquid-phase epitaxies and molecular beam epitaxy were used to prepare B-doped Si samples in order to investigate samples with B concentration in the range between 10^{19} and 10^{21} at/cm^3. B off-lattice displacement is limited by the fluence of excess *Is* per B atom. Small B-*Is* clusters (BICs) were formed as consequence of the interaction with *Is* produced during the ion irradiation. Clusters structures were investigated by simulating the channeling angular scans of cluster configurations predicted by theoretical calculations. In the early stage of *Is* injection, experimental observations are consistent with the presence of the predicted B_2I clusters. These small BICs evolved into different structures under further ion irradiation.

DOI: 10.1103/PhysRevB.81.075210 PACS number(s): 61.72.J−, 61.82.Fk, 61.85.+p, 85.40.Ry

I. INTRODUCTION

The excess of point defects, typically created by ion implantation, is the main cause of B clustering phenomena in crystalline Si. Dopant interaction with Si self-interstitials (*Is*) was pointed out as the origin of transient enhanced diffusion and deleterious dopant deactivation. In fact, it was extensively demonstrated that the presence of a supersaturation of *Is* induces dopant deactivation via the precipitation into electrically inactive Boron-Interstitial-Clusters (BICs).[1–5] Clustering proceeds through the formation of immobile precursors by the usual mechanisms of Si self-interstitial diffusion and B kickout. The precursors of BICs form at concentrations far below the B solubility limit during implantation or in the very early stages of annealing, when Si interstitial supersaturation is very high. Then, they act as nucleation centers for the formation of B-rich clusters during annealing. B-rich clusters constitute the electrically inactive B component, so that the clustering process greatly affects both junction depth and doping level in high-dose implants. A*b initio*[6] and tight binding density functional methods[7,8] were used to calculate the stable configurations of the components of the large BICs family. Referring to the table by Liu *et al.*[6] BICs are cataloged by the number of B atoms and Si atoms in the cluster. The growth path was extensively investigated in order to explain the deactivation mechanism that occurs for several B concentrations, implant and annealing conditions[3,9,10] by using Monte Carlo atomistic simulations. The direct observation of B clusters is an experimental challenge that moves the TEM microscopists to improve the technique,[11,12] but the identification of small complexes is based only on indirect observations[6] and is still unclear. In particular, Pelaz's model[9] is able to reproduce the diffusion profiles of B implanted Si and annealed at temperature about 800 °C, while very few data are available about the clusters that can be formed at lower temperature (<200 °C). According to Liu *et al.*,[6] we expect that large clusters will have higher energy configurations, moreover their formation can be kinetically precluded at low temperature.

Channeling measurements have been widely used to determine the lattice location of foreign atoms in crystals.[13,14] We studied the early stage of B clustering in crystalline Si at room temperature,[15–17] through the detection of the B lattice location that is very sensitive to the formation of simple BIC structures, like the B-B pairs.

In this paper, we review our recent results on BIC formation induced by ion beam irradiation in B-doped Si samples in a wide range of B concentration (10^{19}–10^{21} at/cm^3). At room temperature, B atoms undergo an off-lattice displacement under *Is* supersaturation induced by ion irradiation. The B displacement is limited by the fluence of excess *Is* per B atom and can be described using a simple model of B-*Is* interaction with the formation of small BICs.[15] In the early stage of *Is* injection, the channeling angular scans along the ⟨100⟩ and ⟨110⟩ crystal axes are consistent with the formation of B_2I clusters. The BICs evolution as function of injected *Is* will be discussed in comparison with the predicted growth paths.

The details of the experimental procedure are reported in Sec. I. Experimental results about the B displacement in several samples with different B concentration are reported in Sec. II. First, we show unambiguously that B clustering is caused by the injection of Si point defects, since we implanted Si ions in selected samples where the B-doped layer is spatially separated by the damaged region. Second, the B displacement as a function of the B concentration was studied by using H irradiation. The lattice location of BICs was investigated by performing angular scans along ⟨100⟩ and ⟨110⟩ axes. Angular scans of BICs predicted in literature were simulated by the FLUX code[18] and are reported in Sec. III. The BICs formed as a consequence of ion irradiation were investigated with the help of channeling simulations. The mechanism of the BICs formation under ion irradiation is discussed in comparison with other experimental observations and theoretical predictions. Section IV summarizes our conclusions.

II. EXPERIMENTAL

A. Sample preparation

Samples used in this experiment consist of buried Si:B-doped layer as well as surface doped layer. Several techniques were used to prepare the samples in the required B concentration range. In particular, liquid-phase epitaxy (LPE, a rapid melting and solidification induced by laser irradiation) was applied to get substitutional B well above the solid solubility limit. The details of the sample preparation are listed in the following. In any case the substrate was (100) *n*-type Si substrates (resistivity 4–10 Ω cm).

(1) *MBE samples*: several samples were grown by molecular beam epitaxy (MBE). The first set of samples was prepared by depositing 400-nm-thick Si layer uniformly doped with a B concentration of 1×10^{20} at/cm^3. Buried B-doped layers were produced by sequential deposition of B-doped Si and pure Si. In particular, two different samples with B buried layer (60 nm Si doped with B at 2×10^{20} at/cm^3) were prepared by covering the fresh deposited Si-B layer with 200 and 700 nm of pure Si, respectively (typical Si self-interstitial trapping density is about $\sim10^{16}$ cm^{-3} in undoped MBE Si).[19] A surface doped B-doped Si (2×10^{20} B/cm^3) 60 nm thick was also prepared as reference.

(2) *SPE samples*: $^{11}B^+$ was implanted at RT into substrates previously amorphized by Si implantation at liquid nitrogen temperature (the thickness of the amorphous layer was 550 nm). Multiple energy (17, 29, and 50 keV) implantation was performed in order to have a constant and uniform B-doped layer 400 nm thick at a concentration of 1×10^{20} at/cm^3. Samples were then annealed at 580 °C for 1 h in N_2, to recrystallize Si by solid phase epitaxy (SPE) and to activate the implanted dopant.

(3) *ELA samples*: 1 keV $^{11}B^+$ was implanted in crystalline silicon. Post-implantation Excimer Laser Annealing (ELA) was performed in vacuum at room temperature using a Lambda Physik LPX 205 XeCl excimer laser ($\lambda=308$ nm, 28 ns pulse duration) equipped with a beam homogenizer, forming a 7×7 mm^2 spot on the sample. After ELA with 10 pulses of an energy density of 850 mJ/cm^2, liquid-phase diffusion results in a redistribution of the boron over a region of about 100 nm, with a reasonable uniformity of the B concentration and a good abruptness of the profile edge. The boxlike profile was measured by SIMS (Ref. 17) and maximum B concentration is about 1×10^{20} and 1×10^{21} at/cm^3 for 1×10^{15} and 1×10^{16} cm^{-2} implanted fluences, respectively.

B. Ion Irradiation

Ion irradiation was used to generate Si point defects (vacancies, *Vs*, and interstitials, *Is*) at a controlled rate. The ion mass and energy were changed in order to form *Is* inside or outside the doped region. In particular, irradiation with 650 keV H^+ beam produces *Is* at low rate along the ion track, 20 keV Si beam was used to confine the collision cascade in the 30 nm thick near surface region. In both cases, the beam was randomly impinging at the sample surface, with a 7° tilt angle

C. Characterization

Boron in Silicon cannot be detected by standard Rutherford backscattering spectrometry since the lower atomic number of B with respect of Si. Nuclear Reaction Analysis (NRA) is an ion beam technique to detect B atoms in Si by measuring the yield of α particles from the reaction $^{11}B(p,\alpha)^8Be$, which has a broad resonance near the proton energy of 650 keV.[20,21] channeling effect measurements have been widely used to determine the lattice location of foreign atoms in crystals. By simultaneous measurements of the signals from lattice and foreign atoms, one can determine the crystallographic site location of the foreign atom. To specify site location, it is necessary to measure angular yield profiles along more than one axial direction. NRA and channeling measurements along the ⟨100⟩ and ⟨110⟩ axes were performed using the $^{11}B(p,\alpha)^8Be$ reaction (proton energy of 650 keV)[20,21] on the virgin and irradiated samples. The α particles detector was placed at 160° with respect to the incident beam direction and it was covered with a 10-μm-thick aluminized mylar film to prevent backscattered protons to reach the detector. A second detector, at 165°, was used to detect protons backscattered from Si atoms and to perform the alignment procedure. The normalized channeling yield χ (χ_{Si} and χ_B, for host Si and B atoms, respectively) is defined as the ratio of the aligned yield to the yield of randomly directed beam. χ_B was obtained from the energy integrated α particle yield normalized to the random yield and is proportional to the fraction of B displaced out of lattice, χ_{Si} was measured just below the surface peak of the backscattered proton spectrum (not shown). Angular scans were performed by measuring χ_{Si} and χ_B as a function of the tilt angle swept by the proton beam around a crystal axis (⟨100⟩ or ⟨110⟩) inside the (100) plane. In this description, the angular scan of substitutional impurities appears like a replica of the Si scan with a strong dip at zero tilt, while a random displacement produces a flat angular scan.[21] The uncertainty of χ is statistically determined by the number of counts in the aligned spectrum, the proton and α signals have been acquired in order to have the maximum 5% (3%) error for the minimum χ of B (Si). The uncertainty on the tilt angle is 0.01°. Therefore, in the angular scans shown in the following, the size of symbols accounts for both error bars.

It should be noted that when small BICs are formed, the amount of involved *Is* is on the same order of B atoms per cluster. This means that, for example, to clusterize a B concentration C_B in the cluster B_2I, a *Is* concentration $C_I=C_B/2$ is required. If $C_B\sim10^{21}$ cm^{-3}, it is $C_I\sim5\times10^{20}$ cm^{-3}. The channeling signal of 1% at Si off-lattice displaced is overlaid on the signal from the host crystal causing a maximum increase of χ_{min}(Si) of about 0.01 that is very difficult to detect. On the contrary, the signal of B is not affected by the host crystal and the effect of off-lattice displacement is easier to observe. For this reason, in this work, we will focus only on the B angular scans, being the Si angular scans only weak affected by the presence of BICs.

III. RESULTS

A. Si implantation

Aim of this experiment is to enlighten if substitutional B is affected by point defects generated by ion irradiation in a

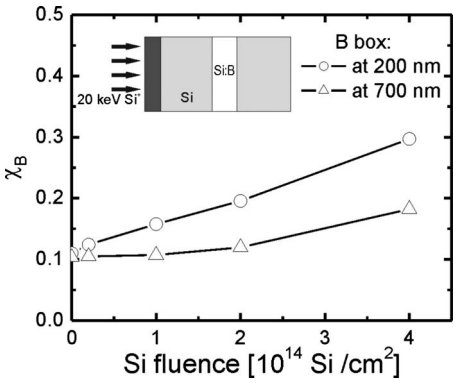

FIG. 1. ⟨100⟩ B channeling yield as a function of 20keV $^{14}Si^-$ ion implanted fluence in samples where the B-doped layer (2×10^{20} B/cm^3) is buried at 200 nm (circles) and 700 nm (triangles) depth (see the schematic).

close by region. This effect can be evidenced by spatially separating the region of B doping from the region where *Is* are generated. For this purpose, the MBE samples with the 60-nm-thick buried B layer (at a depth of 200 and 700 nm under the surface) were implanted at room temperature with 20 keV $^{14}Si^-$ ions at several fluences in the range between 2×10^{13} and 4×10^{14} cm^{-2}. The projected range of Si^- ions, calculated by the SRIM code,[22] resulted Rp=30 nm (ΔRp =10 nm) and about 500 at./ion are displaced along ion tracks. Of course, this is an upper level for *Is* generation since it does not take into account defect recombination, i.e., *Is* annihilation with *Vs*. It is known that the generation of *Is* by ion implantation is efficient only in crystalline Si, for this reason the fluence was maintained well below the amorphization threshold. The damaged region of the Si lattice has been observed in the channeling spectra (not shown) and it is localized in the surface region (<100 nm) well separated from the B-doped region (200 and 700 nm deep from the surface in the two MBE samples, respectively). The measured number of displaced Si atoms is about 3.7×10^{16} cm^{-2} in the sample implanted with a Si fluence of 1×10^{14} cm^{-2}. The χ_{Si} in the B-doped region is about 5% and is almost constant as a function of the Si implanted fluence, which indicates that *Is* migrating from the surface region are not detectable by channeling.

The B channeling yield χ_B along the ⟨100⟩ axis is reported as a function of the implanted Si fluence in Fig. 1. A progressive increase of the χ_B with the irradiation fluence is evident, being such increase smaller with increasing the distance between the surface and the doped layer. The collision cascades of the implanted ions and the B-doped region are spatially separated so that the B displacement cannot be due to direct knock-on or to any direct interaction with the implanted ions. The B displacement in the buried layer can be only the result of the interaction of substitutional B atoms with ion beam generated defects, which migrate and reach the B-doped region. It was demonstrated[23] that ion beam generated *Is* can migrate for distance of the order of few microns even at room temperature. Our experiment clearly shows that the B off-lattice displacement is triggered by the *Is* that reach the doped region, interact with the substitutional B atoms and induce the off-lattice displacement of B atoms. The deeper the doped layer, the smaller the number of *Is* that affect the B lattice location.

B. H irradiation

B off-lattice displacement was measured at room temperature as a function of *Is* fluence produced by H^+ irradiation. H^+ beam energy was 650 keV and fluencies were varied up to 4×10^{17} H^+/cm^2 at a fixed current of 50 nA (further details of this experiment are reported in a previous work).[15] The beam spot was 1 mm^2, and the beam was incident at a random direction on the sample. Each irradiation was followed by *in situ* NRA-channeling measurements. The crystalline quality of the Si lattice was monitored by simultaneously detecting the backscattered protons through a dedicated detector. The proton fluence for each channeling analysis was 5×10^{15} H^+/cm^2, to avoid sample modification during analysis. In a previous work,[24] we reported that the measured B minimum χ_B increases as a function of the displaced Si concentration produced by the 650 keV H^+ beam in a sample doped with B at 1×10^{20} at/cm^3. χ_B increases along the ⟨100⟩ and ⟨110⟩ axes reaching the saturation after irradiation with 8×10^{16} H^+/cm^2 at two different values of $\chi_B^{\langle100\rangle}=0.55$ and $\chi_B^{\langle110\rangle}=0.40$, respectively. This difference suggests that the B off-lattice displacement is not random, but in a specific location. The progressive B off-lattice displacement from substitutional sites is compatible with the formation of mobile pairs B*I*, which migrate in the Si matrix till a stable BIC is formed.[15] The saturation value of $\chi_B^{\langle100\rangle}=0.55$ is stable under further H irradiation. However, after irradiation with H fluence of about 10^{17} at/cm^2, Si displacement is also detectable with a slow increase of the χ_{Si} in the surface region. Moreover, we measured the value of χ_B after the H beam was turned off. The $\chi_B^{\langle100\rangle}$ value slowly decreased from 0.55 to 0.45 in 10 h after the last irradiation. $\chi_B^{\langle100\rangle}=0.45$ has been observed in the irradiated spot 24 h and 10 days after the last irradiation. Moreover, the same sample irradiated until χ_B reaches the value of $\chi_B^{\langle100\rangle}\sim0.45$ is stable 10 days after the last irradiation, so we assume that this configuration with $\chi_B^{\langle100\rangle}\sim0.45$ is stable at room temperature.

We measured the B off-lattice displacement as a function of B doping concentration. In order to vary the B concentration from 1×10^{19} to 1×10^{21} at/cm^3, we used different techniques to dope silicon. MBE and SPE were suitable to prepare samples with B concentration in the range 10^{19}–10^{20} at/cm^3, while LPE was used for B concentration in the range 10^{20}–10^{21} at/cm^3. Samples doped with B at 1×10^{20} at/cm^3 were prepared by every methods in order to test, if any, the effects due to the different sample preparations. All the samples were irradiated with 650 keV H^+ beam as a function of H^+ fluence until the χ_B reaches the value of $\chi_B^{\langle100\rangle}\sim0.45$. Figure 2 reports the ⟨100⟩ χ_B as a function of the H^+ fluence for several B concentrations. The curves referring to B concentration of 1×10^{20} at/cm^3 are almost overlapping, indicating that different sample preparation can only have a negligible effect. Moreover, the χ_B increases faster for the lower B concentration. This is the result of the

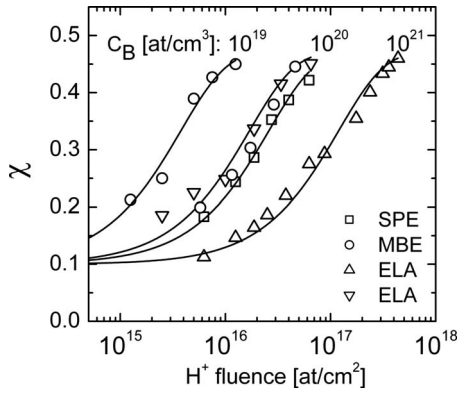

FIG. 2. ⟨100⟩ B channeling yield as function of 650keV H^+ implanted fluence. B dopant concentration is reported in the legend, samples were prepared by using different methods: SPE (squares), MBE (circles), and ELA (triangles). Continuous line is a guide for the eyes.

Is trapping process by the substitutional B atoms; the lower the B concentration the lower the *Is* concentration necessary to displace B atoms from their substitutional location.

The angular scans were performed after the irradiation when χ_B reaches the value of $\chi_B^{\langle 100\rangle} \sim 0.46$. The angular scans of all samples were very similar, χ_B is reported in Fig. 3 for only three samples, thus indicating that the B off-lattice displacement does not depend on B concentration and sample preparation, χ_{Si} is shown only once since it is the same in all the cases. The angular scans along (100) plane of substitutional B in the unirradiated sample have $\chi_{B\,min}^{\langle 100\rangle} \approx 0.11$ and half width $\Psi_{1/2}$, taken at $\frac{1}{2}(1+\chi_{B\,min})$, of about $\Psi_{1/2}^{\langle 100\rangle} \approx 0.43°$ for the ⟨100⟩ axis, and $\chi_{B\,min}^{\langle 110\rangle} \approx 0.07$, $\Psi_{1/2}^{\langle 110\rangle} \approx 0.51°$ for the ⟨110⟩ axis.[25] After irradiation, the minimum χ_B values are $\chi_{B\,min}^{\langle 100\rangle} \approx 0.46$, $\chi_{B\,min}^{\langle 110\rangle} \approx 0.32$, with $\Psi_{1/2}^{\langle 100\rangle} \approx 0.40°$ and $\Psi_{1/2}^{\langle 110\rangle} \approx 0.31°$, respectively. The difference of the angular scans along the two axes (in particular the shrinkage of $\Psi_{1/2}$ along the ⟨110⟩ with respect to the virgin sample) is an indication that B atoms are not randomly distributed in the lattice, but that they occupy specific lattice locations, which can be investigated by channeling. To

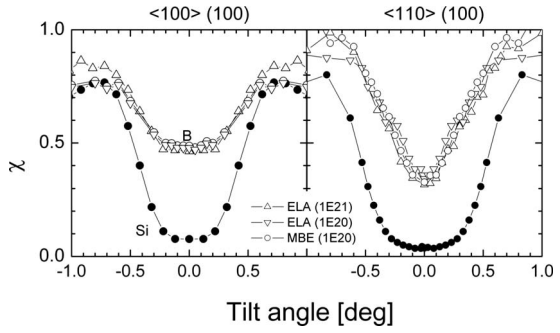

FIG. 3. Angular scans along ⟨100⟩ and ⟨110⟩ axes through the (100) plane measured on the ELA (▽) and MBE (○) B-doped samples at concentration of 1×10^{20} at/cm^3 after 650 keV H^+ irradiation at fluence of 6×10^{16} H/cm^2; and ELA (△) B-doped samples at concentration of 1×10^{21} at/cm^3 after 650 keV H^+ irradiation at fluence of 4×10^{17} H/cm^2. B (Si) signal is indicated by empty (filled) symbols.

this purpose, we examined the different BICs configurations reported in literature and we calculated the angular scans expected from these models, using FLUX code[18] for the simulation of channeling measurements. The calculated angular scans are reported in the following section, they have been used to compare the simulated scans with the experimental ones in order to find out what, among the different theoretical defect configurations, are compatible with experimental observations.

C. Channeling Simulation of BICs

In order to simulate the B angular scans measured in the irradiated samples, we analyzed the proposed defect configurations calculated by *ab initio* methods (Liu *et al.*)[6] and tight binding density functional (DFTB) simulations.[7,8] The DFTB simulations are less accurate than the *ab initio*, but they allow to investigate a large number of different atomic configurations with the same stoichiometry.

Referring to the Liu's table,[6] first, we examine the neutral BICs. We studied clusters that involve few B atoms (≤4) and no more than two Si atoms, since larger agglomerates have angular scans typical of random off-lattice displacement which are not observed here. The FLUX code,[18] based on a Monte Carlo calculation algorithm, was used to simulate the angular scans through different axes (further details about the FLUX code can be found in Refs. 18, 25, and 27). Angular scans on pure Si single crystal allowed to set all the parameters of the simulation (vibrational amplitude of the lattice, beam divergence) in order to match our experimental setup and measurement conditions. The flux distribution of the impinging ions was calculated collecting a large number of those trajectories (about 10000). Suitable and reasonable B sites in the Si lattice were then chosen to calculate the angular scans. Figure 4 reports the scans calculated for different BICs structures. The number of Si atoms located in the interstitial positions inside these small BICs cannot be estimated because it is below the detection limit. Therefore, under our experimental conditions, this technique is only sensitive to the B off-lattice displacement. The uncertainty of simulated B position in the Si crystal cell is about 0.1 Å, the coordinates of B atoms in the BICs have been calculated from the literature references reported in the following.

The B_2I cluster is the simplest and stable complex predicted by *ab initio* and DFTB calculations.[6,7] This defect, named B dumbbell ⟨100⟩ or B-B split ⟨100⟩, is constituted by two B atoms sharing a substitutional lattice site, and it is oriented along the ⟨100⟩ directions. It is characterized by a (calculated) bond length of 1.54 Å (Ref. 7) or 68% of the Si first neighbor distance.[28] It is stable at room temperature, due to its formation energy of about 2 eV.[6] The simulated angular scans along the ⟨100⟩ and ⟨110⟩ axes of the B_2I are showed in Figs. 4(a) and 4(b), respectively.

The angular scans of the B_2I_2 dimer are shown in Figs. 4(c) and 4(d). The cluster consist of a two B atoms, a dumbbell, or a BB dimer located in the middle of the hexagonal ring of the silicon lattice. This defect was calculated the first time by Liu *et al.*,[6] Alippi *et al.*[7] proposed two defects, which differ in the B positions even though they have almost the

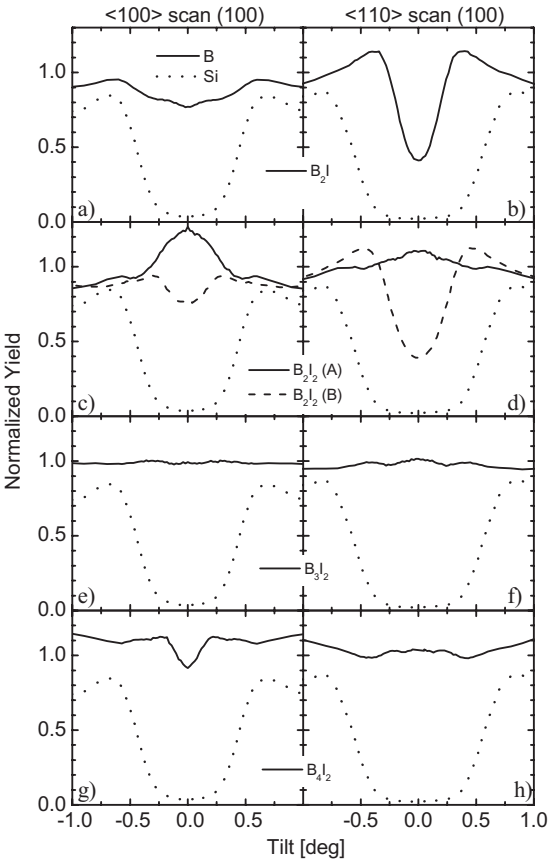

FIG. 4. FLUX simulated B (solid lines) and Si (dotted lines) angular scans along ⟨100⟩ and ⟨110⟩ axes through the (100) plane for various B_xI_y defects: (a–b) B_2I (split ⟨100⟩); (c–d) B_2I_2 with configurations A (solid line) and B (dashed line); (e–f) B_3I_2; (g–h) B_4I_2.

same calculated energy. For the cluster predicted by Liu *et al.*[6] [configuration A in Fig. 4(c) and 4(d)], a flux peaking effect is evident, especially in the ⟨100⟩ angular scan, and is due to the projections of the B atoms in the ⟨100⟩ and ⟨110⟩ flux cells. The other configuration [configuration B in Fig. 4(c) and 4(d)], calculated by Alippi *et al.*,[7] is more symmetrical, it is made up from the two stable single-specie interstitials, the Si-⟨110⟩ and B-⟨100⟩ dumbbells. This structure has a planar geometry and looks like a split ⟨100⟩ that is "distorted" with respect to the ⟨100⟩ axes.

For the B_3I_2 cluster, the χ_B versus the tilt angle is quite flat along both investigated axes [Fig. 4(e) and 4(f)], this kind of scan is very similar to that obtained for random B off-lattice displacement.

The larger defect we considered is the B_4I_2. The configuration is still symmetrical; in fact, it is constituted by two couples of atoms that lie in the same plane. The simulated angular scans of this complex are reported in Figs. 4(g) and 4(h), also in this case, the minimum χ_B is about 1, very similar to the random case.

When different configurations of BICs coexist, the resulting angular scan is the linear sum of the scans relative to each configuration weighted on the relative BIC population. FLUX simulations indicated that BIC with more than two B atoms tend to have a flat angular scans typical of random

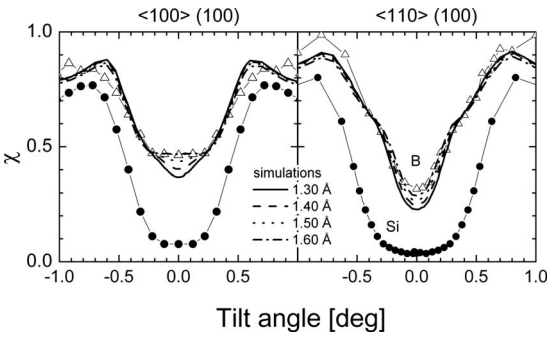

FIG. 5. Angular scans along ⟨100⟩ and ⟨110⟩ axes through the (100) plane measured on the B-doped sample doped with 1×10^{21} B/cm^3 after 650 keV H^+ irradiation: experimental data (symbols) and simulations (lines) of the B_2I (split ⟨100⟩) cluster with several bond length.

displaced atoms. These angular scans with high value of χ_B at zero tilt cannot match our experimental data even if a consistent amount of B atoms is placed into substitutional sites.

Finally, we analyzed the charged BICs. It should be noted that previous work on electrical characterization (Hall effect) showed that hole carrier concentration decreases as function of ion irradiated fluence (see Ref. 26 for details). The doping level associated to charged BICs and their eventual contribution to the total hole carrier concentration and mobility is not reported in literature. However, since the hole carrier concentration decreases as function of ion irradiated fluence, the formation of neutral defects is high probable. Referring to Liu's table, the simulated angular scans along ⟨110⟩ axis (not reported) of BI_3^+ is too narrow with respect to experimental data, indicating that these BICs are not good candidates. BI^+, B_3I^-, and B_4I^- have B atoms in location very close to substitutional sites so they cannot produce such high χ_B observed experimentally at center of ⟨100⟩ angular scans. $B_3I_3^-$, $B_4I_3^-$, and $B_4I_4^-$ are very big clusters and their average angular scans are almost flat, like the scans reported in Fig. 4(e)–4(h).

Finally, we selected two candidates for the final fitting procedure of experimental data: B_2I (split⟨100⟩), B_2I_2 [configuration B in Fig. 4(c) and 4(d)]. The angular scans of the 650keV H^+ irradiated samples of Fig. 3 has been simulated assuming that three configurations of B positions can coexist in the Si lattice, i.e., B atoms can be into BIC complex, or they can be substitutional or random displaced. The simulation of this B distribution can be simply obtained using the property of the χ's linearity, therefore the χ of each configuration is calculated and the resulting χ is determined by adding the singles components weighted on the relative B concentration. The B_2I_2 structure did not result into a good fit, since the width of the ⟨100⟩ angular scan is too narrow with respect to the experimental scan. Figure 5 shows the best fit obtained with the following populations: 45% of the total B concentration is clustered in the B_2I structure, 48% is substitutional and the remaining 7% is in random location. The bond length was varied in the range of 1–2 Å, the simulations in the range 1.3 to 1.6 Å are showed in Fig. 5. The experimental data can be reproduced assuming the formation

of the B_2I defect with a bond length between 1.5 and 1.6 Å, which value is in good agreement with the predicted length of 1.54 Å.

D. Discussion

Our experimental data, in comparison with the channeling simulations indicates clearly that a B off-lattice displacement occurs during ion bombardment and this is related to the formation of BICs. The Si implantation experiment (Fig. 1) shows that B displacement is not induced by the direct ion-B interaction (kickout). Si point defects generated at long distance from the B-doped region can migrate in Si at room temperature, interact with B atoms and induce B diffusion (as demonstrated by Napolitani *et al.*)[29] as well as B clustering. The concentration of *Is* necessary to observe the BICs formation by channeling measurements mainly depends on the B concentrations in the doped layer (Fig. 2), the higher the B concentration the higher the number of *Is* required to completely transform the substitutional boron into BICs. The actual amount of necessary *Is* is not easy to calculate by SRIM simulation since this does not take into account *Is*-vacancies annihilation. By integrating the number of *Is* per ion generated in 400-nm-thick doped region (0.33 *Is*/ion are created by 650 keV H^+ on Si), 2 *Is* per B atoms are evaluated to be necessary to observe $\chi_B^{\langle 100\rangle} \sim 0.45$. However, this number does not take into account *Is* coming from regions outside the B-doped layer, these extra *Is* can migrate and interact with B, as the Si implantation experiment demonstrated.

The comparison of experimental and simulated angular scans strongly suggests that BICs should contain no more than two B atoms. The BIC that is formed in the early stage of damaging (when $\chi_B^{\langle 100\rangle} \sim 0.45$) has different characteristics with respect to the defect observed at the saturation regime (when $\chi_B^{\langle 100\rangle} \sim 0.55$).[15] The angular scan of the early damaging regime can be fitted assuming a distribution of 45% of B atoms in the simple B_2I clusters, while the remaining part prevalently occupies substitutional sites. This is in agreement with electrical data, the substitutional component of about 50%, that is still electrically active, could indicate that the BIC formation is still occurring and the process is not saturated. However, we found that the defect at saturation (when $\chi_B^{\langle 100\rangle} \sim 0.55$)[15] cannot be simulated using the available configurations of BICs and probably it is the result of a mix of different clusters. The difference between the two regimes indicates there is an evolution of the BICs during ion irradiation.

Pelaz *et al.*[9] identified two possible paths for the growth of B clusters, being the predominance of one of the path versus the other determined by the relative stability of the B clusters and the concentrations of B and *I*. In the *low interstitial content* path, new B*i* (interstitial B atoms) are added to pre-existing B clusters, but *Is* are rapidly emitted, leaving B complexes with low interstitial content (B_2I, B_2, B_3I, B_3…). Through this path, B clusters could be formed in the presence of low interstitial supersaturation as long as the B concentration is high enough. The structures of the B_2 and B_3I (in the Liu *et al.* configuration)[6] are not compatible with our experimental data, therefore, an evolution of the simple B_2I cluster into the complex observed at the saturation level seems to be not in agreement with this path of growth or with the structures of the predicted defects. The alternative path involves a *high interstitial content*. In this case, B*i* are added to pre-existing B clusters without *Is* emission. Therefore, B complexes with high interstitial content will be formed (BI_2, B_2I_2, B_3I_3, B_4I_4…). The formation of such complexes is only possible under a high *Is* supersaturation as, for example, during implantation.

Analysis of observed BICs evolution between presaturation (when $\chi_B^{\langle 100\rangle} \sim 0.45$) and saturation regimes (when $\chi_B^{\langle 100\rangle} \sim 0.55$)[15] in comparison with the predicted path of growth is not so straightforward. The predicted paths of Pelaz *et al.*[9] was deduced from experimental data about the B deactivation as function of the *Is* emitted by the dissolution of the end of range defects in the high temperature regime ($T \sim 800$ °C). In our case, the clusters evolution during irradiation could be different because the injection of *Is* is maintained constant through the ion irradiation and the system is at room temperature. Moreover, we observed that the final BICs formed during H irradiation are stable for further *Is* injection, but if the beam is switched off the $\langle 100\rangle$ χ_B decreased from 0.55 to the value of 0.45 in 10 h after the last irradiation. The angular scans confirmed that B configuration changed by evolving into the B_2I observed in the presaturation regime. This effect did not happen in B implanted in crystalline Si,[16] in that case we observed the same angular scan on H^+ irradiated sample but a different path of BICs dissolution as a function of the annealing temperature. BICs evolve into larger BICs in presence of substantial *Is* supersaturation or dissolve (at temperature ~500 °C) if no excess *Is* are sustained. This indicates that the final BIC is stable under high *Is* supersaturation.

The merging of the experimental data and the theoretical predictions can suggest the following scenario.

(1) the B_2I defect is formed in the early stage (when $\chi_B^{\langle 100\rangle} \sim 0.45$) of H^+ irradiation.

(2) When the B channeling yield reaches the saturation level (when $\chi_B^{\langle 100\rangle} \sim 0.55$)[15] another kind of small BIC is detected.[15] This BIC was also observed in B implanted crystalline Si,[16] it cannot be simulated using the available configurations of BICs since it is probably the result of a mix of different small BICs.

(3) Following the growth path of Pelaz *et al.*[9] and the BICs configurations of Liu *et al.*[6] the presaturation defect belongs to the low *Is* path while the saturation complex to the high *Is* path. Therefore, the saturation defect could be a mix of B_2I defects generated during the early stage of *Is* injection and more complex BICs formed when the high *Is* path is switched on by the increasing in the excess *Is*.

IV. CONCLUSIONS

B off-lattice displacement was observed in ion irradiated B-doped Si and is produced by the interaction of B substitutional atoms with the Si point defects created by the ion beam. We showed that channeling technique can be usefully developed to study the early stage of the B clustering when

the flux of ion beam generated- *Is* in the doped region is low (about 2 *Is* per B atom). In this regime, the comparison of simulated and experimental angular scans suggests the formation of simple BICs with no more than two B atoms. Channeling of small BICs was simulated by FLUX, the angular scans of B_2I, B_2I_2, B_3I_2, and B_4I_2 were presented. The fit of the experimental data indicated the B_2I, predicted by *ab initio* calculations, as the best candidate, with a bond length of about 1.6 Å that is in good agreement with the theoretical value. The B lattice displacement increases as a function of the injected *Is* fluence until a saturation level is reached, at which all the B atoms are clustered into small BICs (no more than two B atoms). These final clusters cannot be identified with any calculated structures, probably representing a mix of different small clusters.

ACKNOWLEDGMENTS

The authors wish to thank P. Alippi (CNR-IMM of Catania) for useful discussions, V. Privitera (CNR-IMM of Catania) for the ELA samples, S. Tatì, C. Percolla (MATIS, Catania), and A. Marino (CNR-IMM of Catania) for their technical expertise. This work has been partially supported by MIUR under Project No. PRIN 2004.

[1] W. K. Hofker, H. W. Werner, D. P. Oosthoek, and N. J. Koeman, Appl. Phys. (Berlin) **4**, 125 (1974).
[2] A. Armigliato, D. Nobili, P. Ostaja, M. Servidori, and S. Solmi, in *Semiconductor Silicon*, edited by H. Huff and E. Sirtl (The Electrochemical Society, Princeton, N.J., 1977), Vol. 77-2, p. 638.
[3] L. Pelaz, M. Jaraiz, G. H. Gilmer, H.-J. Gossmann, C. S. Rafferty, D. J. Eaglesham, and J. M. Poate, Appl. Phys. Lett. **70**, 2285 (1997).
[4] A. D. Lilak, M. E. Law, L. Radic, K. S. Jones, and M. Clark, Appl. Phys. Lett. **81**, 2244 (2002).
[5] S. Mirabella, E. Bruno, F. Priolo, D. De Salvador, E. Napolitani, A. V. Drigo, and A. Carnera, Appl. Phys. Lett. **83**, 680 (2003).
[6] X. Liu, W. Windl, and M. Masqueleir, Appl. Phys. Lett. **77**, 2018 (2000).
[7] P. Alippi, P. Ruggerone, and L. Colombo, Phys. Rev. B **69**, 125205 (2004).
[8] J. Adey, J. P. Goss, R. Jones, and P. R. Briddon, Phys. Rev. B **67**, 245325 (2003).
[9] L. Pelaz, G. H. Gilmer, H.-J. Gossmann, C. S. Rafferty, M. Jaraìz, and J. Barbolla, Appl. Phys. Lett. **74**, 3657 (1999).
[10] M. Aboy, L. Pelaz, L. A. Marques, P. Lopez, J. Barbolla, and R. Duffy, J. Appl. Phys. **97**, 103520 (2005).
[11] F. Cristiano, X. Hebras, N. Cherkashin, A. Claverie, W. Lerch, and S. Paul, Appl. Phys. Lett. **83**, 5407 (2003).
[12] S. Boninelli, S. Mirabella, E. Bruno, F. Priolo, F. Cristiano, A. Claverie, D. De Salvador, G. Bisognin, and E. Napolitani, Appl. Phys. Lett. **91**, 031905 (2007).
[13] S. T. Picraux, in *New Uses of Ion Accelerators*, edited by B. J. F. Ziegler (Plenum Press, New York, 1975), Chap. 4.
[14] J. U. Andersen, O. Andreason, J. A. Davies, and E. Uggethoj, Radiat. Eff. **7**, 25 (1971).
[15] A. M. Piro, L. Romano, S. Mirabella, and M. G. Grimaldi, Appl. Phys. Lett. **86**, 081906 (2005).
[16] L. Romano, A. M. Piro, S. Mirabella, M. G. Grimaldi, and E. Rimini, Appl. Phys. Lett. **87**, 201905 (2005).
[17] L. Romano, A. M. Piro, V. Privitera, E. Rimini, G. Fortunato, B. G. Svensson, M. Foad, and M. G. Grimaldi, Nucl. Instrum. Methods Phys. Res. B **253**, 50 (2006).
[18] P. J. M. Smulders and D. O. Boerma, Nucl. Instrum. Methods Phys. Res. B **29**, 471 (1987).
[19] S. Mirabella, A. Coati, D. De Salvador, E. Napolitani, A. Mattoni, G. Bisognin, M. Berti, A. Carnera, A. V. Drigo, S. Scalese, S. Pulvirenti, A. Terrasi, and F. Priolo, Phys. Rev. B **65**, 045209 (2002).
[20] M. Vollmer, J. D. Meyer, R. W. Michelmann, and K. Bethge, Nucl. Instrum. Methods Phys. Res. B **117**, 21 (1996).
[21] J. R. Tesmer and M. Nastasi, *Handbook of Modern Ion Beam Materials Analysis* (Materials Research Society, Pittsburgh, 1995).
[22] J. F. Ziegler, J. P. Biresack, and U. Littmark, *The Stopping and the Range of Ions in Solids* (Pergamon, New York, 1985).
[23] K. K. Larsen, V. Privitera, S. Coffa, F. Priolo, S. U. Campisano, and A. Carnera, Phys. Rev. Lett. **76**, 1493 (1996).
[24] A. M. Piro, L. Romano, P. Badalà, S. Mirabella, M. G. Grimaldi, and E. Rimini, J. Phys.: Condens. Matter **17**, S2273 (2005).
[25] A. M. Piro, L. Romano, S. Mirabella, and M. G. Grimaldi, Mater. Sci. Eng., B **124-125**, 249 (2005).
[26] L. Romano, A. M. Piro, M. G. Grimaldi, and E. Rimini, Nucl. Instrum. Methods Phys. Res. B **249**, 181 (2006).
[27] P. J. M. Smulders, D. O. Boerma, B. Bench Nielsen, and M. L. Swanson, Nucl. Instrum. Methods Phys. Res. B **45**, 438 (1990).
[28] J. Zhu, T. Diaz dela Rubia, L. H. Yang, C. Mailhiot, and G. H. Gilmer, Phys. Rev. B **54**, 4741 (1996).
[29] E. Napolitani, D. De Salvador, R. Storti, A. Carnera, S. Mirabella, and F. Priolo, Phys. Rev. Lett. **93**, 055901 (2004).